PEP GOODS-S data release (v. 1.2)

The PEP GOODS-S data reduction and extraction groups,
with key contributions by:

Stefano Berta (MPE), Benjamin Magnelli (MPE),
Paola Popesso (MPE), Francesca Pozzi (INAF-Bo).

July 5, 2010

1 Contents of the released package

This document describes the content of the *first post-SDP data release of PEP data*. The released package consists in the GOODS-S field and is briefly named *PEP GOODS-S v. 1.0*.

The GOODS-S field has been observed by PACS, using the scanmap mode, and employing a total of 204 AORs. Of these, 96 performed observations in the blue (70 μm) and red (160 μm) channels, while the remaining 108 used the green (100 μm) and red (160 μm) bands. Thus, the effective exposure in the red band is roughly double of the other two channels.
The released package includes:

1. PEP PACS maps,
2. observed PSFs,
3. maps describing the correlated noise,
4. catalogs extracted blindly,
5. catalogs extracted using 24μm position priors,
6. curves for completeness and fraction of spurious sources for the aforementioned catalogs,
7. residual maps,
8. cross-IDs between the PACS blind catalog and the 24 μm (Magnelli et al., 2009) and multiwavelength (MUSIC, Grazian et al., 2006; Santini et al., 2009) catalogs.
9. multiwavelength file, including both flavors of PACS catalogs, 24 μm cross-identifications and deblending flags at 24 μm.

These data do not include significant changes, with respect to SDP v. 2.2. We defer to the SDP v. 2.2 release documentation for details about previous releases.

Here we remind that the latest data reductions are:

- PEP GOODS-S v. 1.2 (this release): including GOODS-S data.
- PEP COSMOS v. 1.1: including COSMOS data.
- SDP v. 2.2: including GOODS-N and Abell 2218 data.

1.1 From v. 1.0 to v. 1.2

This *delta* release includes the full GOODS-S dataset, i.e. vv 1.0 and 1.1 should be considered as superseeded. The main changes with respect to v 1.0 are:

- in PEP GOODS-S version 1.1, we have prepared a multiwavelength file, which includes both flavors of PACS catalogs (blind and extracted with 24 μm priors), linked to the 24 μm catalog and to the GOODS-S MUSIC (Grazian et al., 2006; Santini et al., 2009) catalog with cross-IDs. This file includes also blend-flags for 24 μm objects (i.e. more than one MUSIC object within the 24 μm beam, which are very useful to check for strange behaviurs of your favorite samples.

- in PEP GOODS-S version 1.2 (currently released), we have updated the list of cross-IDs in the blind X-ID file and in the priors catalog, which were affected by a glitch. The multiwavelength file released in v. 1.1 (see item above) was not affected.

- all the rest (maps, catalogs, PSFs, etc) is unchanged. Nevertheless, we release here the full package, so to avoid confusion. All files are renamed, and now labeled "1.2".

1.2 Correction factors

As known, the science maps were obtained by combining all sub-maps together. The maps are provided in units of *pseudo-Jy*, i.e. a temporary flux calibration. This flux scale is basically not properly calibrated in absolute terms and needs to be scaled to *Jy* through equivalent reductions of calibrator stars. Using aperture photometry in a 20 arcsec radius of γDra, αTau, αCma — and assuming an intrinsic $\nu F_\nu = const$ emission — we obtained the following scaling factors:

$g(70\mu\mathrm{m}) = 1.78$
$g(100\mu\mathrm{m}) = 1.46$
$g(160\mu\mathrm{m}) = 1.43.$

These factors are now already included in the science and error maps, as well as in the released catalogs.

Starting from this data release, we apply one single correction factor to the data, accounting for:

- aperture correction from 20 arcsec (as designed into preliminary fluxcal) to total

- corrections for the incorrect content of responsivity v3.

The new correction factors are computed to make PEP data products consistent with the most recent flux calibration derived by the ICC, as summarized in version 1.1 of the *scanmap* AOT release note (PICC-ME-TN-035 1.1 dated Feb 23, 2010) and also captured in v.5 of the responsivity calibration file (see PACS-2058). There is not yet a more detailed documentation. In the following, this is called the "v.5" calibration.

Note that v.5 calibration assumes a reduction which does *not* include steps related to "drift correction". By now this mode of not using drift correction is the official default (see closure of PACS-2031). This is also what we have used in PEP.

The correct conversions to the v.5 system are:

$m(70\mu\text{m}) = 1/1.05$
$m(100\mu\text{m}) = 1/1.09$
$m(160\mu\text{m}) = 1/1.29$

and are within 5% of the combined corrections that we used for SDP (see v. 2.2 release documentation).

These factors are still not included in the science and error maps, and need to be applied to any custom flux measured by PEP users. Anyways, **they are indeed already included in the released catalogs.**

These corrections bring the map to correct "total flux" but do *not* include aperture corrections or PSF corrections that are specific to the extraction process.

1.3 Released maps

As in previous versions, maps are presented into two different formats:

- data cubes: extension [1] is the science map; extension [2] is the error map; extension [3] is currently empty; extension [4] is the coverage map.
- individual science map and error map, to be used with software not able to deal with datacubes.

As usual, "blue", "green" and "red" refer to the 70μm, 100μm and 160μm bands respectively.

2 Correlated noise

The correlation maps describe the effect of correlated noise in a given pixel, coming from projections, drizzling, resampling, stacking and $1/f$ noise. These maps were produced again from the 204 (96, 108) sub-maps and represent the correlation between two pixels according to their relative position in the map and averaged over a large sample number of locations in the map. The values in the correlation map are the correlation with the central pixel, which is assumed to be similar for every pair of science map pixels with the same Δx, Δy.

This correlation needs to be taken into account when integrating the flux over the PSF and error maps. The correlation map gives correlation factors to be used in the computation of the actual noise/error values to be associated to the extracted fluxes. The correlated error propagation for a weighted sum $f(x_1..x_n) = \sum_i^n a_i * x_i$, with correlations $\rho(i,j)$:

$$\sigma_f^2 = \sum_{i,j}^{n} a_i\sigma_i \cdot a_j\sigma_j \cdot \rho(i,j) \quad (1)$$

If the individual pixel errors are uniform, they can be taken out of the sum:

$$\sigma_f = \sigma_{pix} \sqrt{\sum_{i,j}^{n} a_i a_j \rho(i,j)} \tag{2}$$

In the case of non-correlated errors we set $\rho = 1$ for $i = j$ and $\rho = 0$ for $i \neq j$. The ratio $f = \sigma_{f,corr}/\sigma_{f,nocorr}$ between errors with and without taking correlations into account, or the *correction factor* is just a function of the weights a_i (the PSF) and the correlations $\rho(i,j)$ which are read from the correlation map and is independent of the pixel noise. This was tested across the map and even in areas near the edges of the map, the assumtion of uniform errors leads to an error in the correction factor of less than 2%. For the PSF used in flux extraction the correction factors are:

GOODS-S: $f_{blue} = 1.406$
GOODS-S: $f_{green} = 1.423$
GOODS-S: $f_{red} = 1.590$

These correction factors **are already included in the released catalogs, but are not factored into the error map**, since they depend on the PSFs.

3 Observed PSFs

Point Spread Functions (PSFs) were directly derived from the science maps, during the blind source extraction process with the code Starfinder (Diolaiti et al., 2000a,b). A number of pointlike bright sources, as much isolated as possible, were stacked and then normalized to a unit total flux.

The *observed* PSFs thus obtained are limited to a small radius, compared to the total extent of the PSF. This issue is due to the limited S/N ratio in the maps and the scarcity of bright isolated objects. Summarizing, the observed PSF do not include the wings of the PSFs, but only their core.

Independent observations of very bright objects, such as the asteroid Vesta, have provided a better measure of the in-flight PSF for our observing mode (scan map with speed 20"/s). Aperture corrections can be extimated from these Vesta PSFs, by simply accounting for the limited radius in the observed PSFs.

This computation was performed after adapting the Vesta PSF to the width of the GOODS-S observed PSFs (which are broader than perfection mainly because of small pointing errors). We extracted catalogs with both the observed and the Vesta PSFs and verified that the derived fluxes — after including aperture corrections — were consistent to each other within a few percent.

As an example, Figure 1 show the curves of growth for the GOODS-S blue, green and red PSFs, for the observed and Vesta (labelled "library") cases.

Table 1 list the aperture corrections needed when extracting sources using the observed PSFs. **These aperture corrections are already included in the released catalogs.**

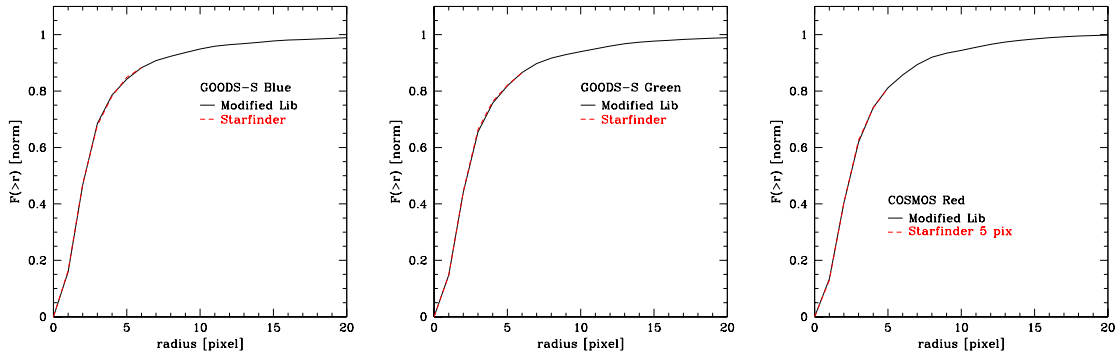

Figure 1: Profiles and curves of growth for GOODS-S observed PSFs, compared to the (libray) Vesta PSFs. Aperture corrections were directly derived from these kind of analysis.

Field	band	radius	Included flux
GOODS-S	blue	6 pix	0.883
GOODS-S	green	6 pix	0.866
GOODS-S	red	5 pix	0.811

Table 1: Aperture corrections to be adopted when using the *observed* PSFs for source extraction

.

4 Blind catalogs

We used the Starfinder IDL code (Diolaiti et al., 2000a,b) to blindly extract the PACS catalogs. We adopted the "direct" noise maps and extracted PSFs directly from the observed maps (see Section 3).

The released catalogs include all sources above a S/N threshold of 3σ, derived directly from the measured fluxes and flux uncertainties.

The average value of the r.m.s. was derived a posteriori on the catalogs, by studying the trend of S/N as a function of flux. An independent extimate has been obtained as part of the extraction with priors (see Section 6) by simply extracting fluxes from 10000 apertures randomly positioned on the (empty) residual map. The two estimates of the r.m.s. are consistent to each other in the blue and green bands, while in the red band, the second value is much higher than the first. This discrepancy is due to the fact that the errors computed within catalogs come from the error map, while the errors computed on residual images include also the *confusion* noise due to sources below the 3σ detection threshold.

It is important to mention that the *direct* error map does not take into account the effects of correlated noise and therefore the output errors on fluxes have been multiplied by the correction factors described in Section 2. **This correction is already included in the released catalogs.**

Table 2 summarizes the main properties of the extracted catalogs.

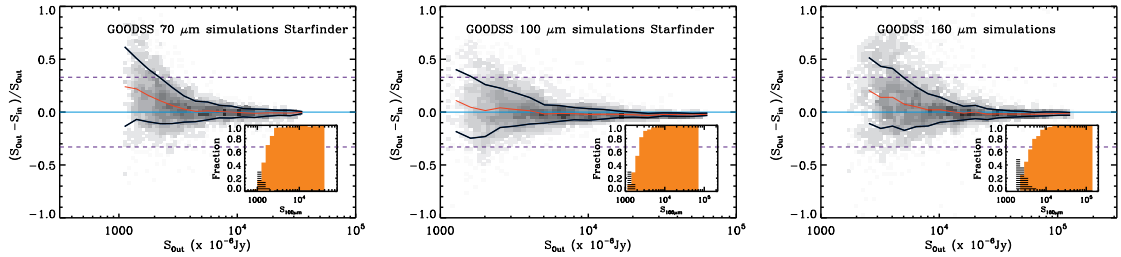

Figure 2: Results of "simulations" in GOODS-S. Comparison of input and output fluxes: red lines represent the average photometric accuracy, blue lines set the standard deviation observed in each flux bin (after 3σ clipping). Orange histograms represent the detection rate (or completeness) computed on the artificial injected sources. Completeness is defined as the fraction of sources that have been detected with a photometric accuracy of at least 50% (Papovich et al., 2004). Black hashed histograms show the fraction of spurious sources, defined as sources extracted above 3σ with an input flux lower than $3\sigma(Image)$.

4.1 Simulations

Up to 10000 artificial sources have beed added to the real PACS final maps, and then extracted with the same Starfinder configuration used for real objects, with the aim to quantify the detection rate (aka in-completeness) and the fraction of spurious detections in the PACS PEP catalogs. Figure 2 shows the results of this analysis and Table 2 includes the completeness and spurious fraction values at the 3σ and 5σ levels.

Despite fine-tuning, Starfinder tends to overestimate the flux of faint sources up to 10-15% at the faintest flux levels, in the blue and red bands, while the green band is almost free from this problem. **A correction of this effect has already been applied to the released catalogs**, using the functions derived from simulations (red lines in Fig. 2). Correction curves are provided in the released data package, in case users would like to un-correct fluxes. Curves of the completeness and the fraction of spurious sources as a function of flux are included as well.

Field & band	F(3σ) mJy	$N \geq 3\sigma$	F(5σ) mJy	$N \geq 5\sigma$	Completeness 3σ	f(spur) 3σ	Completeness 5σ	f(spur) 5σ
GOODS-S 70	~ 1.2	375	~ 2.2	188	0.24	0.26	0.82	0.02
GOODS-S 100	~ 1.2	717	~ 2.0	524	0.06	0.36	0.52	0.03
GOODS-S 160	~ 2.0	867	~ 3.0	646	0.10	0.51	0.38	0.26

Table 2: Statistics of GOODS-S blind catalogs. The 3σ and 5σ flux values of were computed on the S/N vs. flux diagrams.

5 Multi-wavelength cross-IDs

The PACS blind catalogs extracted using Starfinder (see Section 4) have been matched to the GOODS-S 24μm (Magnelli et al., 2009) and multiwavelength MUSIC (Grazian

Bands	number
160+100+70+24	262
160+100+24	516
160+70+24	279
160+24	752
160+100+70	279
160+100	552
160+70	298
160	867
100+70+24	293
100+24	651
100+70	314
100	717
70+24	318
70	377

Table 3: Statistics of maximum-likelihood match in GOODS-S.

et al., 2006; Santini et al., 2009) catalogs by means of a maximum likelihood analysis (Ciliegi et al., 2001; Sutherland & Saunders, 1992), taking advantage of the available 24μm fluxes.

The Magnelli et al. (2009) 24 μm objects have been first matched to MUSIC with a closest-neighbor algorithm, and taking also advantage of the available IRAC (3.6 μm) fluxes. Then these 24 μm objects have been matched to PACS detections using the maximum-likelihood method.

In GOODS-S, the maximum-likelihood method uses a four bands approach, starting from a match between the 160 and 100 μm catalogs, then 70 μm, and finally linking the result to 24 μm.

The maximum-likelihood method takes into account the magnitude distribution of the counterparts and the positional errors of both the sample and the counterpart sample. The formalism of the likelihood ratio technique is described in the full source extraction report.

Cross-IDs are included in the released package. Table 3 summarizes the statistics of the available data.

It is worth to mention that the 24 μm (and multiwavelength) catalog does not cover the entire PACS fields, but is missing the outer areas. Therefore if a given PACS source is not matched to any shorter-wavelength object, it can be either a drop-out or simply out-of-area. Therefore in this case, it is important to check the position of the object (e.g. based on coordinates, or by simply overlaying the position in DS9), in order to understand the reason why a counterpart is missing.

6 Extraction with 24μm priors

In addition to the blind catalogs extracted with Starfinder, we are also providing a catalog obtained using 24μm position priors and PSF-fitting. The catalog with priors

released here is obtained following the Magnelli et al. method and the Magnelli's 24μm source list in GOODS-S.

Table 4 summarizes the properties of the v. 1.0 GOODS-S extracted catalogs. The noise thresholds quoted in this table have been obtained studying the trend of S/N as a function of flux.

6.1 Simulations

Up to 10000 artificial sources have beed added to the real PACS final maps, and then extracted with the same configuration used for real objects, with the aim to quantify the detection rate (aka in-completeness) and the fraction of spurious detections in the PACS PEP catalogs.

The fraction of spurious sources has been derived in two different ways: by blindy extracting from PACS images without any objects (analogous to inverted maps, but obtained by flipping the sign of sub-maps during stacking and hence free of possible artifacts), as well as from simulations (see caption of Fig 3). The two methods lead to consistent results.

Figure 3 shows the results of this analysis and Table 4 includes the completeness and spurious fraction values at the 3σ levels. Curves of the completeness and the fraction of spurious sources as a function of flux are included in the released data package.

6.2 Noise estimate

The Priors extraction provides very clean residual maps, which have been used to estimate the r.m.s. noise value of the PEP GOODS-S data. Fluxes through 10000 apertures randomly positioned on the residual maps were extracted. Figure 4 shows the distribution of the extracted fluxes, peaking around zero, as expected for a well subtracted background, and showing a typical Gaussian profile.

The r.m.s. values derived in this way are roughly consistent to those estimated from the catalogs (i.e. studying the behaviour of S/N as a function of flux) at 70 and 100 μm (see Table 4), as well as to the values obtained from the blind catalogs (see Sect. 4 and Tab. 2).

In the 160 μm band, instead, the value obtained from random extractions is higher than what found directly from catalogs. We believe that this discrepancy is due to the fact that the estimate based on residual images indeed includes also the contribution of *confusion noise*, coming from undetected sources below the 3 σ threshold (which were not subtracted from the science images).

Field & band	F(3σ) mJy	N $\geq 3\sigma$	F(5σ) mJy	N $\geq 5\sigma$	Completeness 3σ	f(spur) 3σ	Completeness 5σ	f(spur) 5σ
GOODS-S 70	~ 1.0	361	~ 1.8	189	0.32	0.21	0.84	0.00
GOODS-S 100	~ 1.1	787	~ 1.9	424	0.21	0.28	0.64	0.04
GOODS-S 160	~ 2.0	874	~ 3.3	531	0.14	0.51	0.52	0.10

Table 4: Statistics of GOODS-S catalogs extracted using position priors at 24μm.

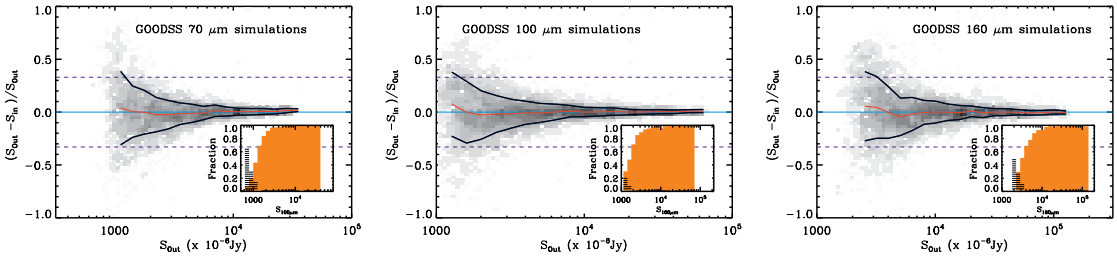

Figure 3: Results of "simulations" in GOODS-S, using 24μm position priors. Comparison of input and output fluxes: red lines represent the average photometric accuracy, blue lines set the standard deviation observed in each flux bin (after 3σ clipping). Orange histograms represent the detection rate (or completeness) computed on the artificial injected sources. Completeness is defined as the fraction of sources that have been detected with a photometric accuracy of at least 50% (Papovich et al., 2004). Black hashed histograms show the fraction of spurious sources, defined as sources extracted above 3σ with an input flux lower than 3$\sigma(Image)$.

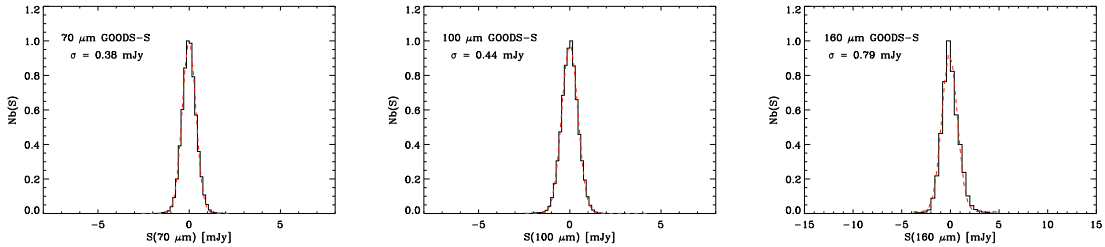

Figure 4: Distribution of fluxes in randomly positioned empty apertures for GOODS-S.

7 Comparison between blind and priors catalogs

A direct comparison between our blind catalogs and our catalogs extracted using 24 mum priors is a good test for data self-consistency. Moreover it is useful also a check for possible mistakes or errors during extraction, calibration, etc.

We briefly report the comparison between the two flavors of catalogs in Figure 5. For each band, we show:

- the direct comparison of fluxes for sources in common to both catalogs;
- the distribution of unmatched sources in absolute number;
- the distribution of unmatched sources in fraction relative to total in the given flux bin.

Fluxes extracted with the two methods (completely independent, excepted for the adopted PSF profiles) are well consistent to each other.

As far as the distribution of un-matched sources is concerned, we find an "excess" of faint objects in the priors catalog, with respect to the blind one. It is actually expected that the catalogs extracted with 24 μm positional priors are deeper than the blind

catalogs and retrieve more faint sources (see also completeness diagrams in Figs. 2 and 3). At 70 and 160 mum, this excess is consistent with the different completeness in the two catalog flavors. On the other hand, at 100 μm, the number of sources in excess is higher than expected on the basis of simulations. Possible explanations are some contamination by spurious sources, a lower detection rate in the blind catalog due to conservative assumptions, or simply a much better performance of the priors method in nearly-confused fields with respect to Starfinder. We will further inverstigate this issue for the next releases.

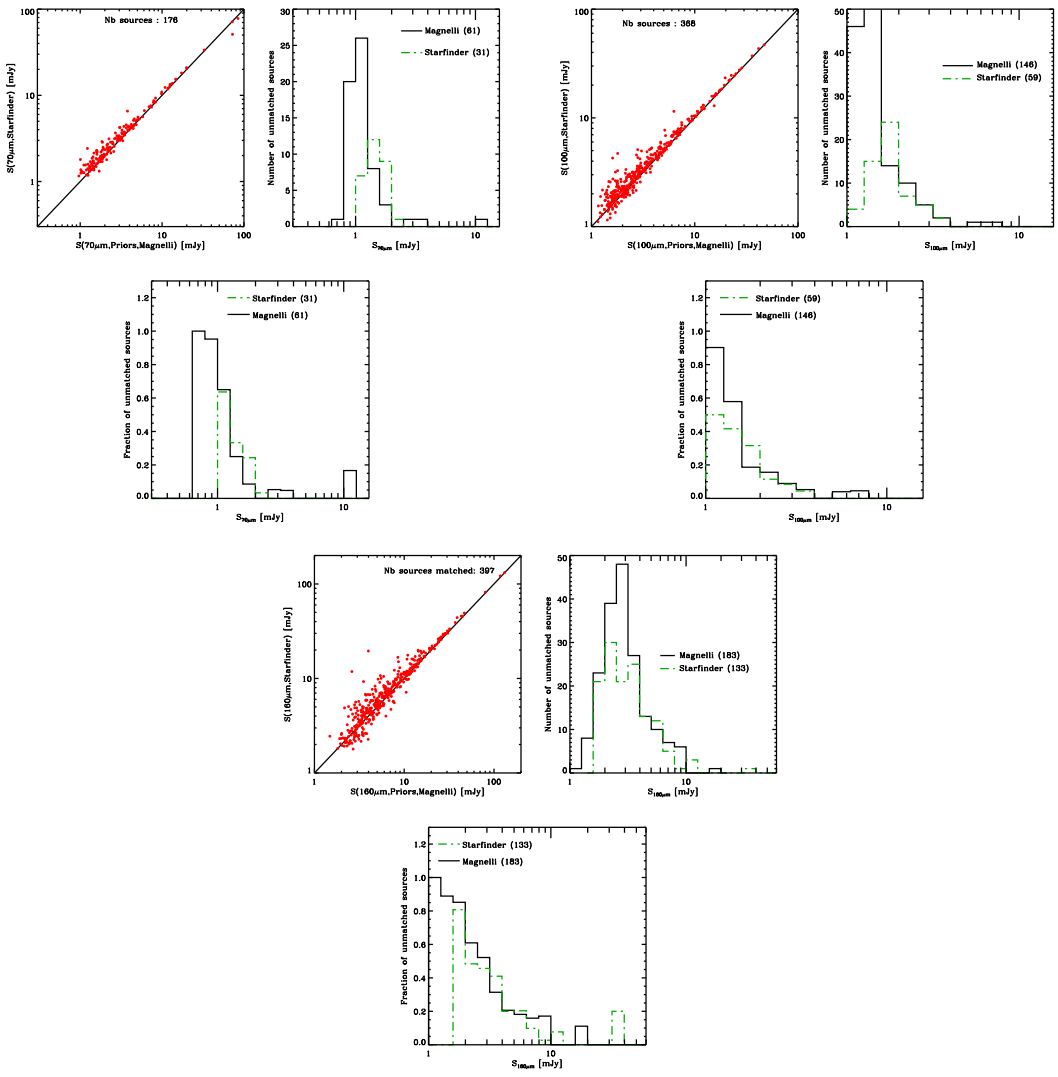

Figure 5: Comparison between blind and priors catalogs in PEP GOODS-S.

References

Ciliegi, P., Gruppioni, C., McMahon, R., & Rowan-Robinson, M., 2001, *Ap&SS*, **276**, 957

Diolaiti, E., Bendinelli, O., Bonaccini, D., Close, L., Currie, D., & Parmeggiani, G., 2000a, *A&AS*, **147**, 335

Diolaiti, E., Bendinelli, O., Bonaccini, D., Close, L. M., Currie, D. G., & Parmeggiani, G., 2000b, in P. L. Wizinowich (ed.), *Society of Photo-Optical Instrumentation Engineers (SPIE) Conference Series*, Vol. 4007 of *Society of Photo-Optical Instrumentation Engineers (SPIE) Conference Series*, pp 879–888

Grazian, A., Fontana, A., de Santis, C., Nonino, M., Salimbeni, S., Giallongo, E., Cristiani, S., Gallozzi, S., & Vanzella, E., 2006, *A&A*, **449**, 951

Magnelli, B., Elbaz, D., Chary, R. R., Dickinson, M., Le Borgne, D., Frayer, D. T., & Willmer, C. N. A., 2009, *A&A*, **496**, 57

Papovich, C., Dole, H., Egami, E., Le Floc'h, E., Pérez-González, P. G., Alonso-Herrero, A., Bai, L., Beichman, C. A., Blaylock, M., Engelbracht, C. W., Gordon, K. D., Hines, D. C., Misselt, K. A., Morrison, J. E., Mould, J., Muzerolle, J., Neugebauer, G., Richards, P. L., Rieke, G. H., Rieke, M. J., Rigby, J. R., Su, K. Y. L., & Young, E. T., 2004, *ApJS*, **154**, 70

Santini, P., Fontana, A., Grazian, A., Salimbeni, S., Fiore, F., Fontanot, F., Boutsia, K., Castellano, M., Cristiani, S., de Santis, C., Gallozzi, S., Giallongo, E., Menci, N., Nonino, M., Paris, D., Pentericci, L., & Vanzella, E., 2009, *A&A*, **504**, 751

Sutherland, W. & Saunders, W., 1992, *MNRAS*, **259**, 413